NJC
New Journal of Chemistry

A journal for new directions in chemistry

Accepted Manuscript

This article can be cited before page numbers have been issued, to do this please use: P. C. Xue, P. Chen, L. Zhang and Z. Yang, *New J. Chem.*, 2019, DOI: 10.1039/C9NJ03881G.

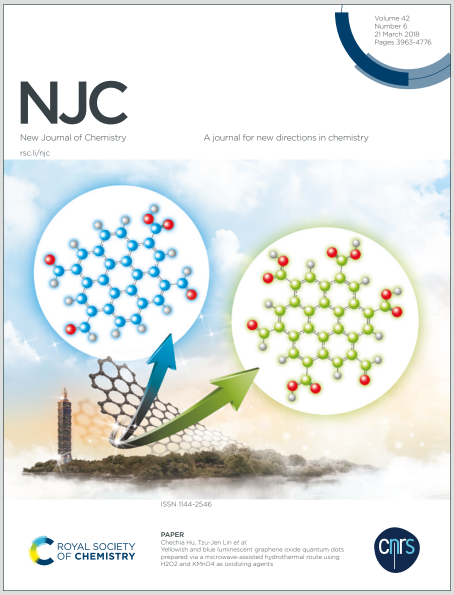

Volume 42
Number 6
21 March 2018
Pages 3963-4776

NJC
New Journal of Chemistry
A journal for new directions in chemistry
rsc.li/njc

ISSN 1144-2546

ROYAL SOCIETY OF CHEMISTRY

PAPER
Chechia Hu, Tzu-Jen Lin *et al.*
Yellowish and blue luminescent graphene oxide quantum dots prepared via a microwave-assisted hydrothermal route using H2O2 and KMnO4 as oxidizing agents

cnrs

View Article Online
DOI: 10.1039/C9NJ03881G

ARTICLE

Received 00th January 20xx,
Accepted 00th January 20xx

DOI: 10.1039/x0xx00000x

Effect of Bridge Unit on Mechanochromism of Phenothiazine-Based Schiff Bases

Zicheng Yang,[a] Pengchong Xue,*[,b] Lulu Zhang,[a] Peng Chen*[,a]

Two phenothiazine derivatives bridged with Schiff base groups have been prepared, and investigation has been taken upon their mechanofluorochromic (MFC) behavior. When the mechanical force is given, the compound PPD (*N*,*N*'-bis(10-ethyl-phenothiazin-2-ylmethylene)-*p*-phenylenediamine) change its color from yellow to orange, exhibiting significant MFC. The reversible MFC behavior of PPD could be accomplished through grinding and fuming with $CHCl_3$. Spectral analysis indicates that PPD molecules are packed in the H-aggregate form in the as-synthesized crystal, whilst it has transformed to the amorphous state under the external grinding. The X-ray analysis reveals that the transfer from the crystalline structure to the amorphous state would respond to the color change. On the other hand, PED (*N*,*N*'-bis(10-ethyl-phenothiazin-2-ylmethylene)-ethylenediamine) with two isolated chromophores does not exhibit MFC behavior, while no phase transition from crystal to the amorphous solid has been found under grinding.

Introduction

Lives are involved in the internal and external stimuli (such as pain, vision, sound) in real time, to which responses are instinctively made for survival. Stimuli-responsive materials, which are spontaneously sensitive and responsible to the external stimuli, have drawn considerable attentions so as to mimic the nature. And the stimuli-responsive organic materials, which are featured by the easy tailoring and multi-functionalities, have the potentials in the applications of data storage, ion recognition, sensing and electronics etc.[1] Therefore, mechanofluorochromic (MFC) materials have been extensively investigated in the recent ten years.[2]

The emission color and intensity of the MFC materials could be altered in response to the discrepant intermolecular interaction under the external stimuli. The external force would collapse or rearrange the stacking in the crystals, resulting in the amorphous state or another crystalline phase.[3] And the grounded sample would emit distinct shifted fluorescence. In most cases, the molecular structure could generally be maintained, although a few examples have revealed the ruins of the chemical bonds for the MFC materials.[4]

Various π-conjugated chromophores and/or functional groups with variable conformations have introduced to assemble the MFC materials that examples are known as triphenylacrylonitrile,[5] tetraphenylethene,[6] 9,10-divinylanthracene,[7] phenothiazine,[8] quinoline[9] derivatives. Some difluoroboron complexes have been reported to demonstrate MFC behavior as well.[10] Meanwhile, full investigations have been drawn on the contribution of length of the alkyl chain, *t*-butyl group and halogen atom etc to address the influence of molecular structure on the MFC performance.[11] As a famous building block for the construction of optoelectronic devices in respect to the push-pull electron structure, phenothiazine is also considerably utilized in the preparation of MFC molecules for its easy functionalization.[12] The non-planar structure of phenothiazine favors to rearrange the molecular packing in the crystal under the external forces, resulting in the MFC molecules.[8,13]

It is noted that the preparation of the organic MFC molecules has often suffered a complex and harsh synthetic condition, which would lead to a low yield in turn. Meanwhile, it remains a challenge to predict the MFC performance of the target molecules. Therefore, a relative easy preparation is obviously favored for the fabrication of MFC materials. Schiff base molecules arisen from the condensation of carbonyl and amine compounds could be easily synthesized under mild condition in a high enough yield.[14] Thus, it is believed it would

---

[a] *Key Laboratory of Functional Inorganic Material Chemistry (MOE), School of Chemistry and Materials Science, Heilongjiang University, Harbin, 150080, P. R. China. Email: jehugu@gmail.com*

[b] *Tianjin Key Laboratory of Structure and Performance for Functional Molecules, MOE Key Laboratory of Inorganic–Organic Hybrid Functional Material Chemistry College of Chemistry, Tianjin Normal University No. 393, Bin Shui West Road, Tianjin, P. R. China. Email: xuepengchong@126.com*

Electronic Supplementary Information (ESI) available: ^1H NMR and ^{13}C NMR spectra, IR spectra, UV-Vis spectra, emission spectra, TG curve and PXRD patterns. See DOI: 10.1039/x0xx00000x

View Article Online
DOI: 10.1039/C9NJ03381G

be a useful strategy to design and synthesize new MFC materials in an easy and high yield way. It is known that the bridge moieties would play key role in the electron distribution. And the introduction of bridge unit in distinct length and conformation would definitely lead to a variation in the structural packing models and the photophysical properties.[15] Two phenothiazine-based Schiff-base derivatives (PED and PPD, Scheme 1) with flexible and rigid bridge units have been prepared, respectively. It is found that PPD assembled with rigid *p*-phenylenediamine as the bridge[16,17] exhibits the MFC behavior, while the compound (PED) connected with ethylenediamine fail to emit the shifted fluorescence under the grinding. PPD has displayed a force-induced color change from yellow to orange that could be reversed by fuming with $CHCl_3$. Further study indicates that the stacking transformation from H-aggregate to the amorphous solid under the external stimuli might be responsible for the MFC performance. The maintenance of crystal phase of PED after grinding should be responsible for its absence of MFC.

Experimental section

Materials and instrumentation

All raw materials were commercially purchased and used without further purification. The ^1H NMR and ^{13}C NMR spectra were recorded on a Bruker Avance III 400 MHz spectrometer at 400 MHz and 100 MHz by using $CDCl_3$ and DMSO-d_6 as the solvents. Elemental analyses were performed on an Elementar Vario EL cube analyzer. FT-IR spectra were recorded on a Perkin-Elmer Spectrum One spectrophotometer by incorporating samples into KBr disks in the experimental range of 4000–370 cm^{-1}. MS detection was performed on an Agilent 6520 Q/TOF mass spectrometer with an ESI source and an AgilentG1607A coaxial sprayer (all from Agilent). X-ray powder diffraction data were collected on a Bruker D5005 X-ray diffractometer with Cu *Kα* radiation in the range of 5-40° (λ = 1.5406 Å). DSC measurements were taken using a NETZSCH STA499F3 QMS403D/Bruker V70 at a heating rate of 10 °C/min under N_2 atmosphere in the temperature range of 25–400 °C. Thermogravimetric analyses were conducted on an SDT Q600 thermogravimetric analyzer at a heating rate of 20 °C/min under air atmosphere in the experimental range of 50–800 °C. Cyclic voltammetry (CV) was obtained on a CHI604C voltammetric analyzer in dichloromethane solution by using Bu_4NBF_4 (0.1 M) as a supporting electrolyte. Platinum plate and platinum wire were used as the working electrode and the counter electrode, respectively. All potentials were recorded versus Ag/AgCl as a reference electrode (using ferrocene as the internal standard). The scan rate was maintained at 100 mV/s. The UV-Vis absorption spectra were obtained by using a Mapada UV-1800pc spectrophotometer. Photoluminescence measurements were obtained on a Cary Eclipse fluorescence spectrophotometer. The fluorescence quantum yields of PPD and PED in toluene solutions were conducted using quinine sulfate in 0.1 M sulfuric acid as a standard. The fluorescence quantum yields of PPD and PED were performed in solid on Edinburgh FLSP920 with the integrating sphere. Geometrical optimization for PPD and PED were performed by density functional theory (DFT) calculations at B3LYP/6-31G(d) level with the Gaussian 09W program package. Electronic transition data obtained by TD-DFT calculation in CAM-B3LYP/6-31G(d) level based on the configuration at ground state.

Syntheses and procedures

10-ethyl-phenothiazine and 10-ethyl-10H-phenothiazine-3-carbaldehyde were prepared and purified according to the reported methods (Scheme S1).[11b,18] The synthetic routes of two compounds were showed in Scheme 1.

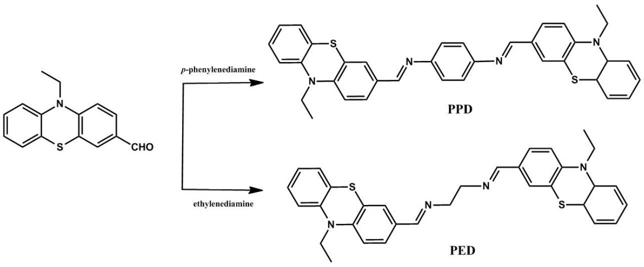

Scheme 1 The synthetic routes and the structures of PPD and PED.

N,N'-bis(10-ethyl-phenothiazin-2-ylmethylene)-*p*-phenylenediamine (PPD)

Firstly, *p*-phenylenediamine (0.54 g, 5 mmol) was added into 20 mL ethanol in 100 mL flask at the room temperature. The above solution was drop-wise added into an ethanol solution (40 mL) of 10-ethyl-10H-phenothiazine-3-carbaldehyde (2.60 g, 10 mmol) under refluxing condition, and precipitate was simultaneously formed. The reaction was allowed to further reflux for 3h, once the titration had been accomplished. And then, the reaction mixture was naturally cooled to the room temperature and the precipitate was collected, washed with ethanol and dried. Yield: 2.66 g, 91 %. mp: 247-249 ˚C. IR (KBr, cm^{-1}): 2975, 2853, 1651, 1596, 1574, 1552, 1496, 1443, 1367, 1325, 1281, 1246, 1192, 1132, 1101, 968, 752. ^1H NMR (400 MHz, $CDCl_3$, 25 ˚C, TMS): δ = 8.37 (s, 2H), 7.69 (s, 2H), 7.65 (d, J = 8.29 Hz, 2H), 7.26 (s, 4H), 7.18 (t, J = 7.55 Hz, 2H), 7.13 (d, J = 8.05 Hz, 2H), 6.97-6.89 (m, 6H), 3.99 (q, J = 6.69 Hz, 4H), 1.47 (t, J = 6.86 Hz, 6H). ^{13}C NMR (100 MHz, $CDCl_3$, 25 ˚C, TMS): δ = 157.98, 149.85, 147.52, 143.87, 130.80, 128.58, 127.43, 127.38, 127.15, 124.58, 123.69, 122.92, 121.81, 115.26, 114.66, 42.21, 12.93. ESI-MS m/z: $[M+H]^+$ 583.1976. Anal. Calcd. (%) for $C_{36}H_{30}N_4S_2$: C, 74.19; H, 5.19; N, 9.62. Found (%): C, 74.20; H, 5.21; N, 9.61.

N,N'-bis(10-ethyl-phenothiazin-2-ylmethylene)-ethylenediamine (PED)

Similar method had been used to prepare PED, except for the addition of ethylenediamine. Yield: 1.98 g, 74 %. mp: 217-219 °C. IR (KBr, cm^{-1}): 2978, 2924, 2860, 1617, 1595, 1575, 1552, 1500, 1463, 1439, 1405, 1371, 1328, 1305, 1284, 1269, 1250, 1190, 1133, 1106. ^1H NMR (400 MHz, DMSO-d_6, 25 ˚C,

View Article Online
DOI: 10.1039/C9NJ03881G

TMS): δ = 8.49 (d, J = 8.66 Hz, 4H), 8.17 (d, J = 7.69 Hz, 2H), 7.87 (dd, J_1 = 1.33 Hz, J_2 = 1.33 Hz, 2H), 7.61 (dd, J_1 = 2.58 Hz, J_2 = 2.14 Hz, 4H), 7.47 (t, J = 7.20, 2H), 7.21 (t, J = 7.62 Hz, 2H), 4.43 (q, J = 7.13 Hz, 4H), 3.94 (s, 4H), 1.30 (t, J = 7.08 Hz, 6H). ^{13}C NMR (100 MHz, DMSO-d_6, 25 °C, TMS): δ = 162.72, 141.41, 140.50, 127.97, 126.59, 125.95, 122.71, 122.64, 121.25, 121.01, 119.77, 109.89, 109.67, 61.80, 37.60, 14.16. ESI-MS was not obtained because PED was easily decomposed. Anal. Calcd. (%) for $C_{32}H_{30}N_4S_2$: C, 71.87; H, 5.66; N, 10.48;. Found (%): C, 71.89; H, 5.67; N, 10.47.

Results and discussion

Photophysical properties in solutions

The UV-Vis absorption spectra of the two compounds in toluene were recorded. As shown in Fig. 1, a maximum peak at 287 nm was found in PED toluene solution, and few weak peaks from 330 to 360 nm were found. Two absorption bands at approximately 290 and 410 nm were observed for PPD. The former band was contributed to the local π-π* transition, while the latter band was ascribed to an extensive π-conjugation structure.

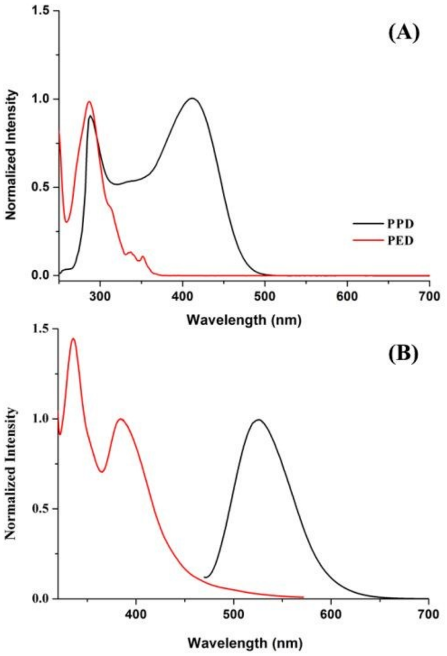

Fig. 1 UV-Vis absorption (A) and fluorescence (B) spectra of PED and PPD in toluene (concentration: 1.0 × 10^{-5} M, λ_{ex}= 300 nm for PED, λ_{ex}= 420 nm for PPD).

To further understand the difference between the two compounds in the absorption spectra, quantum chemical calculations were performed. Firstly, their optimal geometries were obtained by the energy optimization. As shown in Fig. 2, the phenothiazine and imine groups in PED and PPD were almost coplanar. The twisted angles between the central phenyl unit and imine groups were quite small in PPD, while larger twisted angles between the central ethyl group and imine moieties in PED were observed. As it was well-known, the smaller twisted angle among the phenyl rings and imine groups indicated a significant potential for a better π-conjugation. TD-DFT calculations were used to obtain the electron transition, and the results were listed in Table 1. The electron transition of PED gave an absorption peak at 360.95 nm, which was mainly originated from the transition from HOMO to LUMO. Its HOMO was mainly located at phenothiazine moieties, while LUMO density was decreased at the phenothiazine unit and increased at the imine moieties. The results indicated that the central ethyl group prevented π-conjugation of two terminal moieties. The calculated absorption peak of PPD was located at 449.47 nm, and it was ascribed to the transition from HOMO to LUMO. The density distribution change of HOMO and LUMO of PPD suggested that an intramolecular charge transfer excited state in PPD. These results indicated that PPD indeed had a larger π-conjugation, which had induced a longer absorption wavelength. Electrochemical measurements were performed as well to further understand the effect of the bridging unit (Fig. S8). As shown in Table S1, PED had a lower HOMO and higher LUMO energy levels in comparison with PPD. And the larger π-conjugation induced PDD to possess a higher HOMO and a decreased LUMO, which led to a red-shifted absorption band.

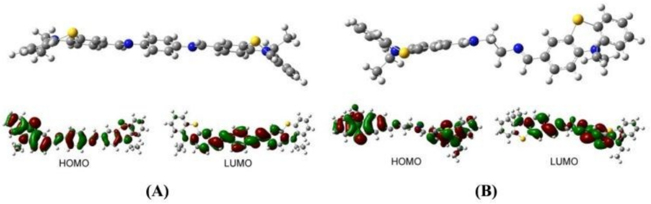

Fig. 2 Optimal configurations and frontier orbitals of PPD (A) and PED (B).

Figure 1B showed the emission spectra of PPD and PED. A maximum emission peak of PPD was located at 525 nm in toluene solution. PED gave two emission maxima at 335 and 384 nm in toluene solution. The shorter emission wavelength of PED was in agreement with its localized π-conjugation. In addition, DFT calculation suggested that the emission of PPD at 525 nm might be arisen from the intramolecular charge transfer (ICT). To confirm it, solvent-dependent fluorescence spectra of PPD were measured. As shown in Fig. S9, the cyclohexane solution had a maximum at 502 nm, which shifted to 525 nm in toluene solution. And the maximum peak was found at 556 nm in polar CH_2Cl_2, exhibiting the orange fluorescence. The result revealed that the molecule PPD had a larger polarity in the excited state than that in the ground state in accordance with the ICT emission.[8a,8c,19]

Mechanochromic behavior

The crystals of PPD were collected as the reaction was naturally cooled to the room temperature, while it was well-

View Article Online
DOI: 10.1039/C9NJ03881G

known that Schiff base molecules were poorly dissolved in ethanol. The crystals were yellow and gave yellow fluorescence. Mortar and pestle were used to finely grind the obtained crystals, and an orange powder was collected. Then, the fine powder was exposed to $CHCl_3$ vapor for a few seconds, the orange color quickly turned to yellow as the grinding was not taken (Fig. 3A). The fluorescence quantum yield changed from 27 % for the pristine to 25 % for the grounded solid.

Table 1. Photophysical data of two compounds in toluene and from quantum chemical calculations (λ_{ex}= 300 nm for PED, λ_{ex}= 420 nm for PPD).

	λ_{abs} (nm)	λ_{em} (nm) (Φ_F)	Absorption extinction coefficient (cm^{-1} L mol^{-1})	Electron transition		Transition assignment	Oscillator strength
				(eV)	(nm)		
PED	287, 354	335, 384 (0.21)	0.10x10^5	3.4349	360.95	HOMO-1→LUMO+1 (23.93%) HOMO→LUMO (67.07%)	PED
PPD	290, 410	525 (0.63)	0.38 x10^5	2.7584	449.47	HOMO-1→LUMO+1 (2.13%) HOMO→LUMO (95.17%)	PPD

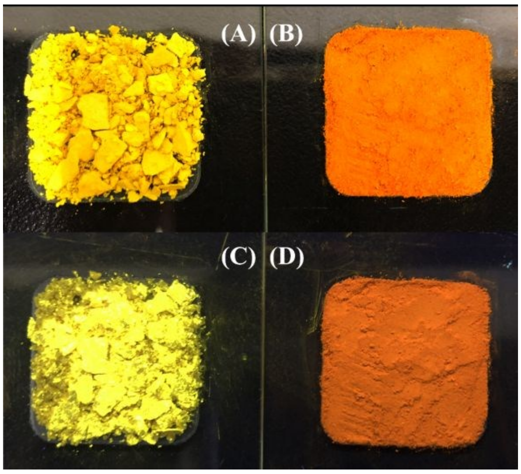

Fig. 3 Photos of PPD solid before (left) and after (right) grinding under (A, C) natural and (B, D) 365 nm light.

The fluorescence change could be repeatedly processed that a reversible MFC performance was obviously detected.[8b] We resorted to the fluorescence and UV-Vis spectra to further study the color change of the ground and fumed samples. As shown in Fig. 4, the crystals collected from ethanol exhibited a maximum emission at 543 nm, whose fluorescence color was yellow (Y-form) as could be seen with naked eyes. The emission wavelength was altered from 543 nm to 567 nm, once the mechanical force had been applied. And the fluorescence color of the ground samples was orange (O-form). When the ground crystals had been exposed to the vapor of $CHCl_3$ for a few seconds, the color of the samples was quickly turned to yellow. And similar emission spectrum could be found as what it was for the un-ground crystals. Once again, the color could be orange, when the fumed samples had been mechanically ground. Such transformation could be reversible for many times under the mechanical and gas stimuli. The ^{1}H NMR spectrum of the O-form solid was obtained and compared with that of the un-ground Y-form, indicative of the consistence. The result confirmed that the mechanical grinding had not ruined the chemical structure in the grinding-fuming cycles.

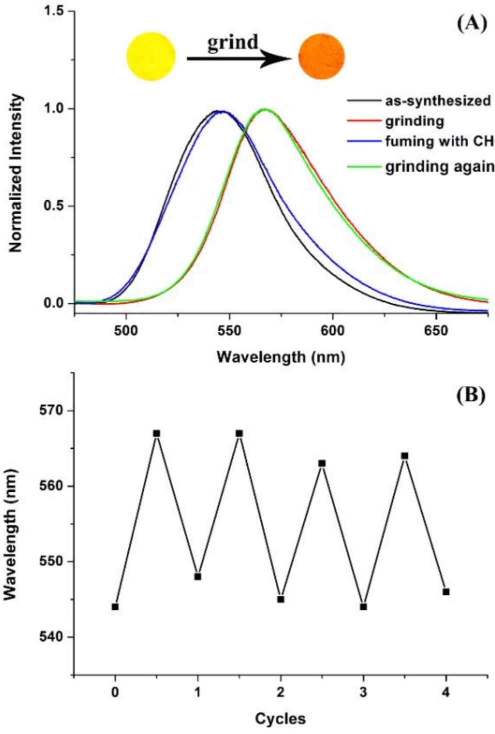

Fig. 4 Normalized fluorescence spectra of PPD (A) in the solid state at different states and (B) the maximum fluorescence emission upon grinding and fuming with $CHCl_3$, repeatedly. Inset: photos of PPD in response to the grinding and fuming.

Mechanofluorochromism had been achieved as it was discussed in the context. We turned to further study the UV-Vis spectra of the as-synthesized and ground samples (Fig. 5).

View Article Online
DOI: 10.1039/C9NJ03881G

The as-synthesized crystals of PPD exhibited a wide absorption with a maximum of 372 nm. It was blue-shifted compared with the maximum peak in cyclohexane solution (400 nm), revealing a face-to-face H-aggregate. The O-form solid had a red-shifted absorption band with a maximum of 415 nm. It revealed that the grinding upon the crystals had significantly destroy H-aggregate in pristine solid.

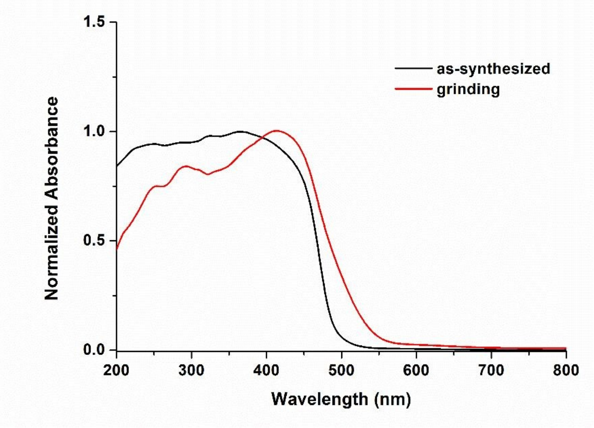

Fig. 5 UV-Vis absorption spectra of PPD in the as-synthesized and ground states.

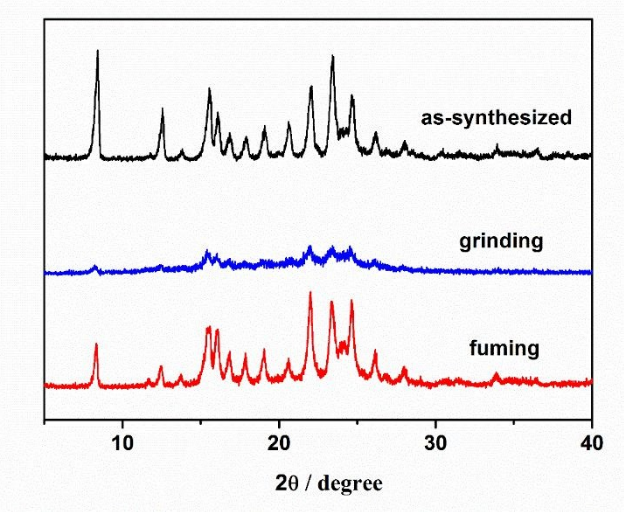

Fig. 6 XRD patterns of PPD in different solid states.

To further study the phase transition during the MFC process, powder X-ray diffraction patterns of PPD were collected. Crystalline was confirmed as sharp peaks were obviously seen in the experimental range of 5-40 degree for the as-synthesized sample of PPD (Fig. 6). The diffraction peaks of the ground PPD were weakened and some weak peaks in the as-synthesized solid disappeared. The results revealed that the ordered stacking was impaired and the ground solid was in an amorphous state. Moreover, the diffraction intensity can be recovered through fuming with $CHCl_3$ and the diffraction peaks were similar to those of the as-synthesized solid, which proved the regeneration of the Y-form solid. This result also suggested that the reversible MFC process of PPD could be achieved in respect to the transfer between the crystalline and the amorphous states.[20]

Thermogravimetric analysis suggest their better heat stability (Fig. S10 and S11). In addition, orange fluorescence of ground solid could be restored to yellow one, when the ground solid was heated at 180 °C for 60 seconds. Differential scanning calorimetry (DSC) measurements were performed to investigate the phase transition induced by the thermal annealing.[10a,21] The DSC curve (Fig. 7) of the pristine PPD exhibited only a single endothermal peak at 248 °C, corresponding to its melting point. However, the ground powders of PPD showed a new exothermal transition peak at 173 °C, indicative of a distinct phase to the as-synthesized crystals. This exothermal peak can be assigned to the cold-crystallization process, implying that that the ground solid was in a metastable state. Under heating, the molecular thermal motion was intensified to prompt the crystals in a more stable phase, resulting in the fluorescence recovery.

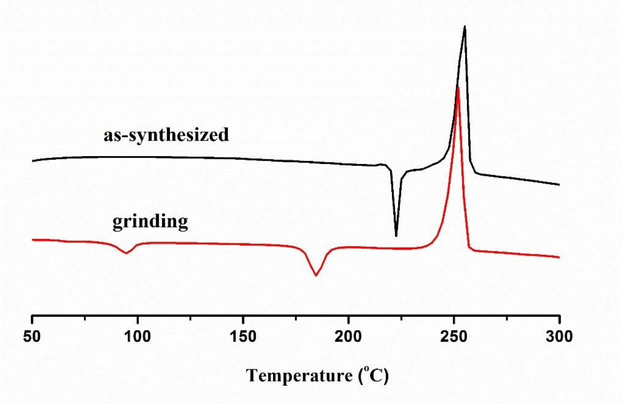

Fig. 7 DSC thermograms of the as-synthesized PPD crystals and the ground PPD powder under nitrogen atmosphere at a heating rate of 10 °C/min.

Once ethylenediamine was employed instead of *p*-phenylenediamine, PED could precipitate as yellowish crystals from ethanol as well (Fig. S12). The as-synthesized crystals emitted strong blue fluorescence under 365 nm light, but fluorescence color change was not observed, implying the absence of MFC. It was noted that no distinct shifts were observed in the UV-Vis absorption and emission spectra of the ground product in comparison with the pristine as-synthesized crystals (Fig. S13), which further confirmed the absence of MFC behavior. The fluorescence quantum yield of PED in toluene solution was 0.21, which was smaller than that of PPD. XRD patterns were collected to study the potential phase transition after grinding. However, the diffraction peaks of ground powder were almost kept unchanged in comparison with the as-synthesized samples (Fig. S14). The above results clearly illustrated that the mechanical force stimuli did not promote a phase transition and the conversion of π-stacking, which might be responsible for the unchanged fluorescence after grinding.

Conclusions

Two Schiff base phenothiazine derivatives with distinct bridge units had been prepared and characterized, and the effects of bridging unit on the photophysical and MFC behavior had been investigated. MFC behavior was observed for PPD with a rigid and conjugated bridge, while no MFC had been detected for PED with a flexible and poorly conjugated bridge. The results indicated that a larger conjugated would have contributed to the MFC performance.

Conflicts of interest

There are no conflicts to declare.

Acknowledgements

This work was financially supported by the Foundation of Development Program of Future Expert in Tianjin Normal University (WLQR201804) and the Science &Technology Development Fund of Tianjin Education Commission for Higher Education (2018ZD12).

Notes and references

1 (a) X. Li, S. Zhang, Y. Dang, Z. Liu, Z. Zhang, D. Shan, X. Zhang, T. Wang and X. Lu, *Anal. Chem.,* 2019, **91**, 4031;
(b) L. Wang, D. Chen, K. Jiang and G. Shen, *Chem. Soc. Rev.*, 2017, **46**, 6764;
(c) T. Li, Y. Li and T. Zhang, *Acc. Chem. Res.,* 2019, **52**, 288;
(d) Y. Liu, K. He, G. Chen, W. R. Leow and X. Chen, *Chem. Rev.*, 2017, **117**, 12893.
(d) H. Lee, M. Kim, I. Kim and H. Lee, *Adv. Mater.,* 2016, **28**, 4541.
(e) Y. Zhang, J. Sun, G. Zhuang, M. Ouyang, Z. Yu, F. Cao, G. Pan, P. Tang, C. Zhang and Y Ma, *J. Mater. Chem. C,* 2014, **2**, 195.
(f) Y. Hou, Z. Li, J. Hou, P. Shi, Y. Li, M. Niu, Y. Liu and T. Han, *Dyes Pigments*, 2018, **159**, 252.

2 (a) S. Matsumoto, J. Moteki, Y. Ito and M. Akazome *Tetrahedron Lett.*, 2017, **58**, 3512;
(b) J. Jia and Y. Wu, *Dyes Pigments,* 2017, **136**, 657;
(c) P. Rajamalli, P. Gandeepan, M. Huang and C. Cheng, *J. Mater. Chem. C,* 2015, **3**, 3329;
(d) P. Xue, P. Wang, P. Chen, B. Yao, P. Gong, J. Sun, Z. Zhang and R. Lu, *Chem. Sci.*, 2018, **8**, 6060;
(e) P. Gong, H. Yang, J. Sun, Z. Zhang, J .Sun, P. Xue, and R. Lu, *J. Mater. Chem. C*, 2015, **3**, 10302;
(f) Z. Yang, Z. Chi, Z. Mao, Y. Zhang, S. Liu, J. Zhao, M. P. Aldred and Z. Chi, *Mater. Chem. Front*., 2018, **2**, 861.

3 (a) J. Zhang, H. Kang, N. Li, S. Zhou, H. Sun, S. Yin, N. Zhao and B. Tang, *Chem. Sci*., 2017, **8**, 577;
(b) Z. Zhang, Z. Wu, J. Sun, B. Yao, P. Xue and R. Lu, *J. Mater. Chem. C*, 2016, **4,** 2854.

4 (a) K. Oda, S. Hiroto and H. Shinokubo, *J. Mater. Chem. C,* 2017, **5**, 5310;
(b) Z. Ma, Z. Wang, X. Meng, Z. Ma, Z. Xu, Y. Ma and X. Jia, *Angew. Chem. Int. Ed.*, 2016, **55**, 519.

5 W. Yuan, Y. Tan, Y. Gong, P. Lu, J. W. Y. Lam, X. Shen, C. Feng, H. H-Y. Sung Y. Lu, I. D. Williams, J. Sun, Y. Zhang and B. Tang, *Adv. Mater.*, 2013, **25**, 2837.

6 (a) Q. Lu, X. Li, J. Li, Z. Yang, B. Xu, Z. Chi, J. Xu and Y. Zhang, *J. Mater. Chem. C,* 2015, **3**, 1225;
(b) Y. Wang, D. Xu, H. Gao, Y. Wang, X. Liu, A. Han, C. Zhang and L. Zang, *Dyes Pigment,* 2018, **156**, 291.

7 J. Zhao, Z. Chi, Z. Yang, Z. Mao, Y. Zhang, E. Ubba and Z. Chi, *Mater. Chem. Front.,* 2018, **2**, 1595.

8 (a) C. Arivazhagan, P. Malakar, R. Jagan, E. Prasad and S. Ghosh, *CrystEngComm,* 2018, **20**, 3162.
(b) P. Xue, B. Yao, J. Sun, Q. Xu, P. Chen, Z. Zhang and R. Lu, *J. Mater. Chem. C,* 2014, **2**, 3942;
(c) Y. Shen, P. Chen, J. Liu, J. Ding and P. Xue, *Dyes Pigments*, 2018, **150**, 354.

9 Y. Shen, P. Xue, J. Liu, J. Ding, J. Sun and R. Lu, *Dyes Pigments*, 2019, **163**, 71.

10 (a) J. Sun, W. Chen, F. Wu, X. Bai, W. Du, L. Fang, Y. Wu, X. Wen, H. Wang and X. Ba, *Dyes Pigments,* 2019, **162**, 808;
(b) Z. Zhang, Z. Wu, J. Sun, B. Yao, G. Zhang, P. Xue and R. Lu, *J. Mater. Chem. C*, 2015, **3**, 4921;
(c) M. Liu, L. Zhai, J. Sun, P. Xue, P. Gong, Z. Zhang, J. Sun and R. Lu, *Dyes Pigments,* 2016, **128**, 271;
(d)M. Yamaguchi, S. Ito, A. Hirose K. Tanaka and Y. Chujo, *Mater. Chem. Front.***,** 2017,**1**, 1573.

11 (a) C. Ma, X. Zhang, L. Yang, Y. Li, H. Liu, Y. Yang, G. Xie, Y. Ou and Y. Wei, *Dyes Pigments*, 2017, **136**, 85;
(b) J. Jia and Y. Wu, *Dyes Pigments*, 2017, **147**, 537;
(c) P. Xue, J. Sun, P. Chen, P. Gong, B. Yao, Z. Zhang, C. Qian and R. Lu, *J. Mater. Chem. C,* 2015, **3**, 4086;
(d) P. Xue, C. Zhang, K. Wang, M. Liang and T. Zhang, *Dyes Pigments*, 2019, **163**, 516;
(e) B. Roy, M. C. Reddy and P. Hazra, *Chem. Sci.*, 2018, **9**, 3592.

12 (a) G. Zhang, J. Sun, P. Xue, Z. Zhang, P. Gong, J. Peng and R. Lu, *J. Mater. Chem. C*, 2015, **3**, 2925;
(b) P. Xue, B. Yao, X. Liu, J. Sun, P. Gong, Z. Zhang, C. Qian, Y. Zhang and R. Lu, *J. Mater. Chem. C,* 2015, **3**, 1018.

13 J. Jia and H. Zhao, *Tetrahedron Lett.,* 2019, **60**, 252.

14 (a) Z. Ma, Y. Ji, Y. Lan, G. Kuang and X. Jia, *J. Mater. Chem. C*, 2018, **6**, 2270;
(b) P. Chen, M. Zhang, W. Sun, H. Li, L. Zhao and P. Yan, *CrystEngComm*, 2015, **17**, 5066;
(c) X. Zhang, J. Shi, G. Shen, F. Gou, J. Cheng, X. Zhou and H. Xiang, *Mater. Chem. Front.***,** 2017, **1**, 1041.

15 (a) T. Watabe, K. Ishizuki, D. Aoki and H. Otsuka, *Chem. Commun.,* 2019, **55**, 6831;
(b) T. Ishi-i, H. Tanaka, R. Youfu, N. Aizawa, T. Yasuda, S. Kato and T. Matsumoto, *New J. Chem.*, 2019, **43**, 4998;
(c) H. Yu, J. Zhi, Y. Shen, W. Ding, X. Zhang and J. Wang, *J. Mater. Chem. C,* 2019, doi: 10.1039/c9tc01772k.

16 (a) L. Esrafili, V. Safarifard, E. Tahmasebi, M. D. Esrafili and A. Morsali, *New J. Chem.,* 2018, **42**, 8864;
(b) V. Safarifard, S. Rodríguez-Hermida, V. Guillerm, I. Imaz, M. Bigdeli, A. A. Tehrani, J. Juanhuix, A. Morsali, M.

View Article Online
DOI: 10.1039/C9NJ03881G

E. Casco, J. Silvestre-Albero, E. V. Ramos-Fernandez and D. Maspoch, *Cryst. Growth Des.,* 2016, **16**, 6016.

17 S. Gopi and M. Kathiresan, *Polymer*, 2017, **109**, 315.

18 F. Hideo and Y. Jun, *J. Heterocycl. Chem.*, 1980, **17**, 1053.

19 a) Z. Zhang, Z. Wu, J. Sun, P. Xue and R. Lu, RSC Adv., 2016, **6**, 43755;
b) Y. Han, H. Cao, H. Sun, Y. Wu, G. Shan, Z. Su, X. Hou and Y. Liao, *J. Mater. Chem. C,* 2014, **2**, 7648.

20 (a) J. Sun, J. Sun, W. Mi, P. Xue, J. Zhao, L. Zhai and R. Lu, *New J. Chem.,* 2017, **41**, 763;
(b) E. V. Fedorenko, A. G. Micochnik, A. V. Gerasimenko, A. Y. Beloliptsev and E. B. Merkulov, *Dyes Pigments*, 2018, **159**, 557;
(c) Z. Ma, X. Meng, Y. Ji, A. Li, G. Qi, W. Wu, B. Zou, Y. Ma, G. Kuang and X. Jia, *Dyes Pigments*, 2019, **162**, 136.

21 P. Xue, Q. Xu, P. Gong, C. Qian, Z. Zhang, J. Jia, X. Zhao and R. Lu, *RSC Adv.,* 2013, **3**, 26403.

View Article Online
DOI: 10.1039/C9NJ03881G

Mechanofluorochromism of Schiff-based phenothiazine derivatives

Zicheng Yang[a], Pengchong Xue[b,*], Lulu Zhang[a], Peng Chen[a,*]

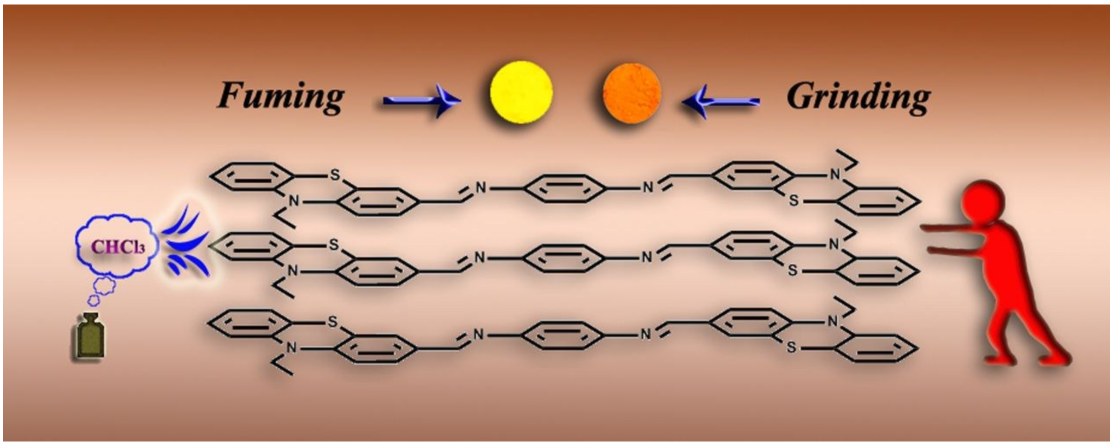

Schiff-based phenothiazine derivatives bearing ethylenediamine and *p*-phenylenediamine have been prepared. Molecule PDD bridged with rigid *p*-phenylenediamine unit show reversible mechanofluorochromism, but one with ethylenediamine did not change its fluorescence after grinding.